Carbohydrate Polymers 92 (2013) 1887–1895

Contents lists available at SciVerse ScienceDirect

Carbohydrate Polymers

journal homepage: www.elsevier.com/locate/carbpol

Fabrication of dual-responsive cellulose-based membrane via simplified surface-initiated ATRP

Xiaoyun Qiu, Xueqin Ren*, Shuwen Hu**

Department of Environmental Sciences & Engineering, College of Resources & Environmental Sciences, China Agricultural University, Beijing 100193, PR China

ARTICLE INFO

Article history:
Received 20 September 2012
Received in revised form
22 November 2012
Accepted 26 November 2012
Available online 3 December 2012

Keywords:
Cellulose membrane
Dual-responsive
Heterostructure
ARGET ATRP

ABSTRACT

An independently temperature- and pH-responsive membrane was developed by simultaneously grafting poly(*N*-isopropylacryamide) (PNIPAAm) and poly[(2-(diethylamino)ethyl methacrylate] (PDEAEMA) from different sides of a crosslinked cellulose membrane. The synthesis was simplified by using surface-initiated activators regenerated by electron transfer for atom-transfer radical polymerization in a diffusion device. The grafted membrane was heterostructured. The grafted polymer layer thickness was linearly related to reaction time. The wettabilities of the double-membrane sides responded individually and reversibly to temperature and pH. The surface grafted with PNIPAAm shifted from hydrophilicity to hydrophobicity above the lower critical solution temperature. The PDEAEMA side was hydrophilic in acidic aqueous solution and hydrophobic under basic conditions. This dual-response cellulose membrane has potential applications in water treatment, separations, and other membrane applications.

1. Introduction

Stimuli-responsive polymers have gained considerable interest because of their fast and reversible structural and morphological transformations in response to surrounding stimulus changes. These polymers are used in the fabrication of stimuli-responsive membranes, which exhibit abrupt property changes such as pore size or surface wettability (Lin, Missirlis, Krogstad, & Tirrell, 2012; Lue, Hsu, & Wei, 2008; Pan, Ren, Li, & Cao, 2012; Tokarev & Minko, 2009; Zhao, Nie, Tang, & Sun, 2011) as a result of their sensitive behaviors in response to environmental changes such as temperature, pH, and ionic strength.

Membranes with responsive properties are promising for a range of applications, including drug delivery (Chen, Wu, Guo, Xin, & Li, 2011; Lue et al., 2008; Lue et al., 2011), separation (Pan, Hamad, & Straus, 2010; Pan, Zhang, Ren, & Cao, 2010; Xiong, Duan, Zou, He, & Zheng, 2010), biosensor (Tokarev & Minko, 2009), and water treatment (Cai, Gorey, Zaky, Escobar, & Gruden, 2011; Wandera, Wickramasinghe, & Husson, 2011), and multi-responsive membranes are preferred in many situations because their property changes in response to multiple stimuli. Drug delivery systems with multi-responsive properties, including temperature/pH, pH/ionic strength, and temperature/magnetic field responses, are suitable for insulin delivery and site-specific delivery of anticancer drugs to tumor sites (Gordijo et al., 2011; Kaiden, Yuba, Harada, Sakanishi, & Kono, 2011). In the water separation and treatment industries, temperature, pH, and ionic strength are among the key factors that can influence membrane performance. Multi-responsive membranes have therefore been built to improve separation capacity (Wang, Zhang, Ji, Qin, & Liu, 2010), antifouling, and cleaning performance (Wandera et al., 2011). Among them, cellulose based membranes have been extensively studied with responsive properties have been widely exploited (Lindqvist et al., 2008; Wang, Tan, et al., 2011; Wang, Qiu, et al., 2011; Xiong et al., 2010) in the applications of anion exchange, separation, controlled release, water treatment, etc. (Liu, Zeng, Tao, & Zhang, 2010; Lqbal, Kim, Yang, Baek, & Yang, 2007; Pan, Hamad, et al., 2010; Pan, Zhang, et al., 2010; Schmitt, Granet, Sarrazin, Mackenzie, & Krausz, 2011; Wu et al., 2010). Being a natural polymer, cellulose is a renewable resources and possessing excellent mechanical strength and suitable modifications can result in improved performance (Qiu, Tao, Ren, & Hu, 2012). However, double-side modifications have never been reported before, and no exceptional for cellulose based membrane.

Presently, stimuli-responsive membranes have been extensively studied, there is still scope for further exploitation of multi-responsive membranes (Kaiden et al., 2011; Shaikh et al.,

Abbreviations: ARGET ATRP, activators regenerated by electron transfer for atom-transfer radical polymerization; ATR-IR, attenuated total reflectance infrared spectroscopy; bpy, 2,2′-bipyridyl; BriB, α-bromoisobutyryl bromide; CCM, crosslinked cellulose membrane; DMAc, *N*,*N*-dimethylacetylamide; DMF, *N*,*N*-dimethylformamide; MCC, microcrystalline cellulose; LCST, lower critical solution temperature; PDEAEMA, poly(2-(diethylamino)ethyl methacrylate); PNIPAAm, poly(*N*-isopropylacryamide); py, pyridine; SEM, scanning electron microscopy; TDI, toluene diisocyanate; THF, tetrahydrofuran; XPS, X-ray photoelectron spectroscopy.

* Corresponding author. Tel.: +86 10 62733407; fax: +86 10 62731016.
** Corresponding author. Tel.: +86 10 62731255; fax: +86 10 62731016.
E-mail addresses: renxueqin@cau.edu.cn (X. Ren), shuwenhu@cau.edu.cn (S. Hu).

0144-8617/$ – see front matter.
http://dx.doi.org/10.1016/j.carbpol.2012.11.080

2010; Wang et al., 2010). There are several methods of fabricating multi-responsive membranes from stimuli-responsive polymers. Alginate-gel membranes with sub-micrometer pores were prepared by salt-induced phase-separation of sodium alginate and gelatin (Gopishetty, Roiter, Tokarev, & Minko, 2008). The membrane had a range of functions mimicking natural skin, and most of the functions were regulated by pH and ionic strength. Zhang, Song, Ji, Wang, and Liu (2008) developed a polyelectrolyte multi-layer membrane on a hydrolyzed polyacrylonitrile hollow fiber membrane using a dynamic negative-pressure layer-by-layer technique. The morphology and pervaporation selectivity for ethanol/water were highly dependent on salt concentration, pH, and oxidant. A layer-by-layer technique was also used by Allen et al. to fabricate glass-supported assembly membranes that responded to solute and temperature (Allen, Tan, Fu, Batteas, & Bergbreiter, 2012). A hybrid polymer membrane was prepared by casting a mixture of poly(ether sulfone) and an amphiphilic block polymer of Pluronic F127-b- poly(2-(diethylamino)ethyl methacrylate) (PDEAEMA) (Yi et al., 2010). The added Pluronic F127-b-PDEAEMA endowed the poly(ether sulfone) membrane with smart properties which responded to temperature and pH stimuli. Grafting techniques are intriguing methods for fabricating stimuli-responsive membrane brushes, since the stimuli-responsive polymers are able to graft from/onto the membrane surface efficiently, and the mechanical strength of the membrane is maintained (Lue et al., 2011). This advantage is of vital importance for membrane industries, especially for water treatment and separation (Cai et al., 2011; Lue et al., 2011), because robust membranes are required in these industries.

One of the most promising methods for grafting membrane brushes is surface-initiated atom-transfer radical polymerization (ATRP). ATRP initiators are first immobilized on the membrane, and responsive polymers are then grafted consecutively in a multi-step process (Lindqvist et al., 2008; Pan et al., 2012; Zhang, Zhu, Xu, Neoh, & Kang, 2009). The advantage of the ATRP technique is that it has the potential to tailor membrane properties, e.g., by enabling adjustment of the grafted polymer thickness, and can be carried out in aqueous solutions under mild conditions. The fabrication of multi-responsive membranes by surface-initiated ATRP typically requires multiple steps after immobilization of ATRP initiators on the membranes. The fabrication of each responsive grafting layer comprises polymerization and purification steps (Pan et al., 2012; Zhang et al., 2009). Adding one more step therefore leads to an inevitable loss of a small, but not negligible, amount of reactive polymer chains, accompanied by formation of polymeric impurities (Schmid, Weidner, Falkenhagen, & Barner-Kowollik, 2012; Weiss & Laschewsky, 2012). Also, multi-polymerization is labor-intensive. It is worth noting that ATRP is a redox-initiated polymerization reaction; the transition metal is susceptible to reaction with oxygen or other oxidizers, and the activity of the metal is quenched after exposure to oxidizers. ATRP polymerization therefore requires an oxygen-free environment throughout the entire process, and specific equipment and critical operations are necessary.

To simplify the preparation of dual-responsive membranes and obtain a novel heterostructured dual-responsive membrane, a diffusion device was used to fabricate dual-responsive cellulose membranes by surface-initiated activators regenerated by electron transfer (ARGET) ATRP in the present work. ARGET ATRP was developed to enable reactions to be conducted under a limited oxygen atmosphere by adding reducing agents, and it overcomes the limitations mentioned above (Matyjaszewski, Coca, Gaynor, Wei, & Woodworth, 1998; Matyjaszewski, Dong, Jakubowski, Pietrasik, & Kusumo, 2007; Matyjaszewski, Tsarevsky, et al., 2007). ARGET ATRP has been used elsewhere to prepare membrane adsorbers (Bhut, Conrad, & Husson, 2012). In this work, an ATRP initiator was first immobilized on a crosslinked cellulose membrane (CCM) prepared according to our previous work (Qiu et al., 2012), and then PNIPAAm and PDEAEMA were simultaneously grafted from each surface of the membrane in one step. The prepared membrane was heterostructured, one surface grafted with PNIPAAm and the other surface grafted with PDEAEMA. The chemical structures of the membrane brushes were characterized by attenuated total reflectance infrared spectroscopy (ATR-IR) and X-ray photoelectron spectroscopy (XPS) to verify the fabrication of dual-responsive cellulose membranes. The morphologies and thicknesses of the grafting layers were observed by scanning electron microscopy (SEM). The dual-responsive behaviors were characterized by contact angle measurements. This work aims to offer a simple method of preparing heterostructured dual-responsive membranes for water treatment, separation industry, and other membrane industries.

2. Experimental

2.1. Materials

Microcrystalline cellulose (MCC) with a degree of polymerization of 210–240, lithium chloride monohydrate (LiCl), and *N*,*N*-dimethylacetylamide (DMAc) were purchased from Sinopharm Chemical Reagent Co., Ltd. (Shanghai, China). Toluene diisocyanate (TDI) was purchased from Shenyang Chemical Reagent Factory (Shenyang, China) and used as received. MCC was dried in an air-drying oven overnight at 80 °C before use. LiCl was dried in a vacuum-oven at 200 °C for 2 h prior to use. *N*-isopropylacryamide (NIPAAm), 2-(diethylamino) ethyl methacrylate (DEAEMA), CuBr, α-bromoisobutyryl bromide (BriB), and 2,2′-bipyridyl (bpy) were obtained from Aladdin Chemistry Co., Ltd. (Shanghai, China). Copper powder (Cu), pyridine (py), *N*,*N*-dimethylformamide (DMF), methanol, tetrahydrofuran (THF), and *n*-hexane were purchased from Sinopharm Chemical Reagent Co., Ltd. (Shanghai, China). NIPAAm was recrystallized from *n*-hexane three times, dried under a vacuum at ambient temperature, and stored at −4 °C for further use. DEAEMA was passed through a column of neutral alumina to remove the inhibitor and stored at −4 °C. THF, DMF, and py were distilled prior to use. All other reagents were purchased from Beijing Chemical Reagents Company (Beijing, China) and used without any pretreatment. Distilled water was used for all the experiments.

2.2. Preparation of crosslinked cellulose membranes

Crosslinked cellulose membranes were prepared according to our previous work (Qiu et al., 2012). Briefly, MCC was dissolved in a solution of DMAc/LiCl, and TDI was added to the cellulose solution. The solution was cast onto a Teflon plate after thorough stirring and dried in an oven at 80 °C overnight. The obtained membrane was washed to remove the LiCl residues and the CCM with TDI weight ratio of 1.30 (TDI/MCC) was obtained after drying at 80 °C for 4 h.

2.3. Preparation of macroinitiator BriB–CCM

The CCM of 2 cm diameter was immersed in DMF/py solution (1:1, v/v) in a three-necked flask, degassed, and recharged with N_2. The flask was incubated in ice-water, and excessive BriB was added drop-wise with a syringe. The ice-water bath was removed after all the BriB was added and the reaction continued for another 4 h at 25 °C. The prepared membranes were washed successively with THF, THF/water (1:1, v/v), methanol, and water, and then soaked in water overnight before ultrasonic washing for 10 min to remove the residues. Finally, the BriB-grafted CCM (BriB–CCM) was dried at 60 °C for 24 h before use.

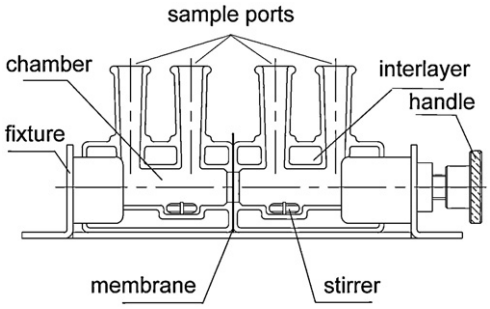

Fig. 1. Diffusion cells of transdermal diffusion device TK-6H.

2.4. Grafting of N-isopropylacrylamide and 2-(diethylamino) ethyl methacrylate on BriB–CCM

ARGET ATRP was used to prepare the dual-responsive cellulose membrane in a TK-H6 transdermal diffusion device from Shanghai KaiKai Science and Technology Trade Co., Ltd. (Shanghai, China). The diffusion device was made up of six diffusion cells attached to a multi-stirrer with fixtures. Each diffusion cell consisted of two detachable glass chambers with two sampling ports, a stirrer, and an interlayer (Fig. 1). BriB–CCM was sandwiched between two chambers with an effective diffusion area of 3.14 cm^2 and sealed with high-vacuum insulating silicone grease. CuBr (4×10^{-5} mol), Cu (1×10^{-3} mol), and bpy (1.2×10^{-4} mol) were added to each chamber. NIPAAm (4×10^{-3} mol) dissolved in 6 mL of methanol was added to one of the chambers and DEAEMA (4×10^{-3} mol) mixed with 5.2 mL of methanol was added to the other chamber. The sampling ports were plugged with rubber plugs, and the interlayer was connected to a thermostatic water bath. The reaction was conducted with circulating water at 40 °C and a stirring speed of 300 rpm. The reaction was stopped at regular intervals by removing the plugs and exposing the catalyst to air. The obtained PNIPAAm- and PDEAEMA-grafted BriB–CCM (PDEAEMA–CCM–PNIPAAm) was washed successively with THF, THF/water (1:1, v/v), methanol, and water, and soaked in water overnight before ultrasonic washing for 20 min to remove the remaining reactants and free polymers. The PDEAEMA–CCM–PNIPAAm was dried at 60 °C for 24 h. The reaction route is shown in Scheme 1.

In order to clarify the penetration effect of the NIPAAm and DEAEMA monomers on the structure of the membrane, monomers were grafted from a single surface. NIPAAm or DEAEMA and the other reagents were added to one of the two chambers, and Cu, CuBr, bpy, and methanol were added to the other chamber with no NIPAAm or DEAEMA; polymerization was conducted at 40 °C for 24 h. The purification method was the same as that described above for PDEAEMA–CCM–PNIPAAm. These membranes are referred to as PDEAEMA–CCM (DEAEMA added to one chamber) and CCM–PNIPAAm (NIPAAm added to one chamber).

2.5. Characterization methods

The chemical structure of PDEAEMA–CCM–PNIPAAm was determined by ATR-IR and XPS. ATR-IR spectra were recorded in the range 675–4000 cm^{-1} with a resolution of 8 cm^{-1} on a Nicolet NEXUS-470 FT-IR spectrometer (Madison, WI, USA). The XPS data were obtained using an AXIS Ultra instrument from Kratos Analytical (Manchester, UK). The anode voltage and current were 20 keV and 10 mA under a pressure of 6.67×10^{-6} Pa, with a take-off angle of 45° with respect to the sample surface. The surface and cross-section morphologies of the membranes were examined by SEM using a JEOL JSM 5400 scanning microscope (JEOL Co., Ltd., Tokyo, Japan) at an accelerating voltage of 15 kV. Samples were mounted on metal stubs and coated with gold–palladium using a Denton Vacuum Desc II (Moorestown, NJ, USA).

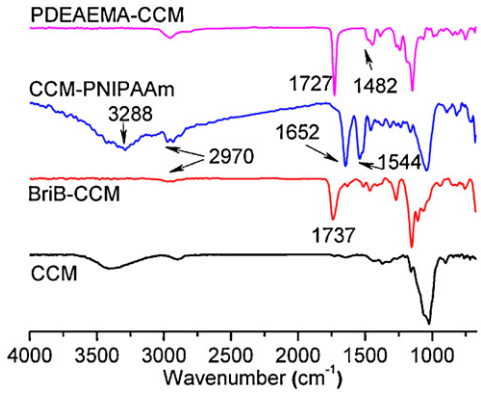

Fig. 2. ATR-IR spectra for TDI-crosslinked cellulose membrane (CCM), BriB-immobilized CCM (BriB–CCM), and PDEAEMA–CCM–PNIPAAm membrane. CCM–PNIPAAm represents the surface grafted with PNIPAAm, and PDEAEMA–CCM represents the other surface, grafted with PDEAEMA.

Contact angles were determined by the pendant drop method with a water drop of volume 3 μL using an optical contact angle meter (SL 100B) from Solon Information Technology Co., Ltd. (Shanghai, China) at room temperature and ambient humidity. All contact angles were measured on both sides of the drop by the ellipse-fitting calculation method. Contact angles were measured at 20 °C, 50 °C, and 80 °C for the surface with grafted PNIAAm and measured at pH values of 1.0, 4.0, 7.0, and 10.0 for the surface with grafted PDEAEMA. The pH values of water were adjusted with HCl and NaOH. Each contact angle was the average value of a minimum of four measurements.

3. Results and discussion

3.1. ARGET ATRP in diffusion device

Conventional multi-responsive membrane brushes are block polymers grafted successively from/onto a membrane surface (Lindqvist et al., 2008; Pan et al., 2012; Zhang et al., 2009), and this method needs multi-step polymerization. The present work used a diffusion device (Fig. 1) to fabricate multi-responsive membrane brushes. The two chambers of the device were separated by the BriB–CCM membrane, and NIPAAm and DEAEMA monomers were added separately to one of the two chambers. The polymerizations of NIPAAm and DEAEMA could therefore be conducted

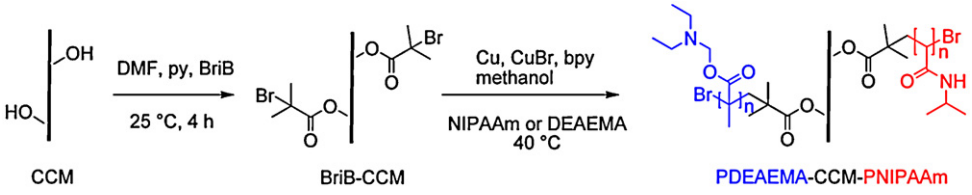

Scheme 1. Surface-initiated ARGET ATRP of PDEAEMA–CCM–PNIPAAm from crosslinked cellulose membrane.

independently on different membrane surfaces, and a heterostructured dual-responsive membrane, PDEAEMA–CCM–PNIPAAm, was obtained in two steps (Scheme 1). Different polymer brushes could be obtained by altering the monomers added to the chambers, making it easy to incorporate different properties into the membrane.

The ARGET ATRP method allows polymerization to proceed with limited oxygen (Matyjaszewski et al., 1998; Matyjaszewski, Dong, et al., 2007; Matyjaszewski, Tsarevsky, et al., 2007), and this avoids the complex deoxygenation operations and using compression devices needed in conventional ATRP. The other advantage of

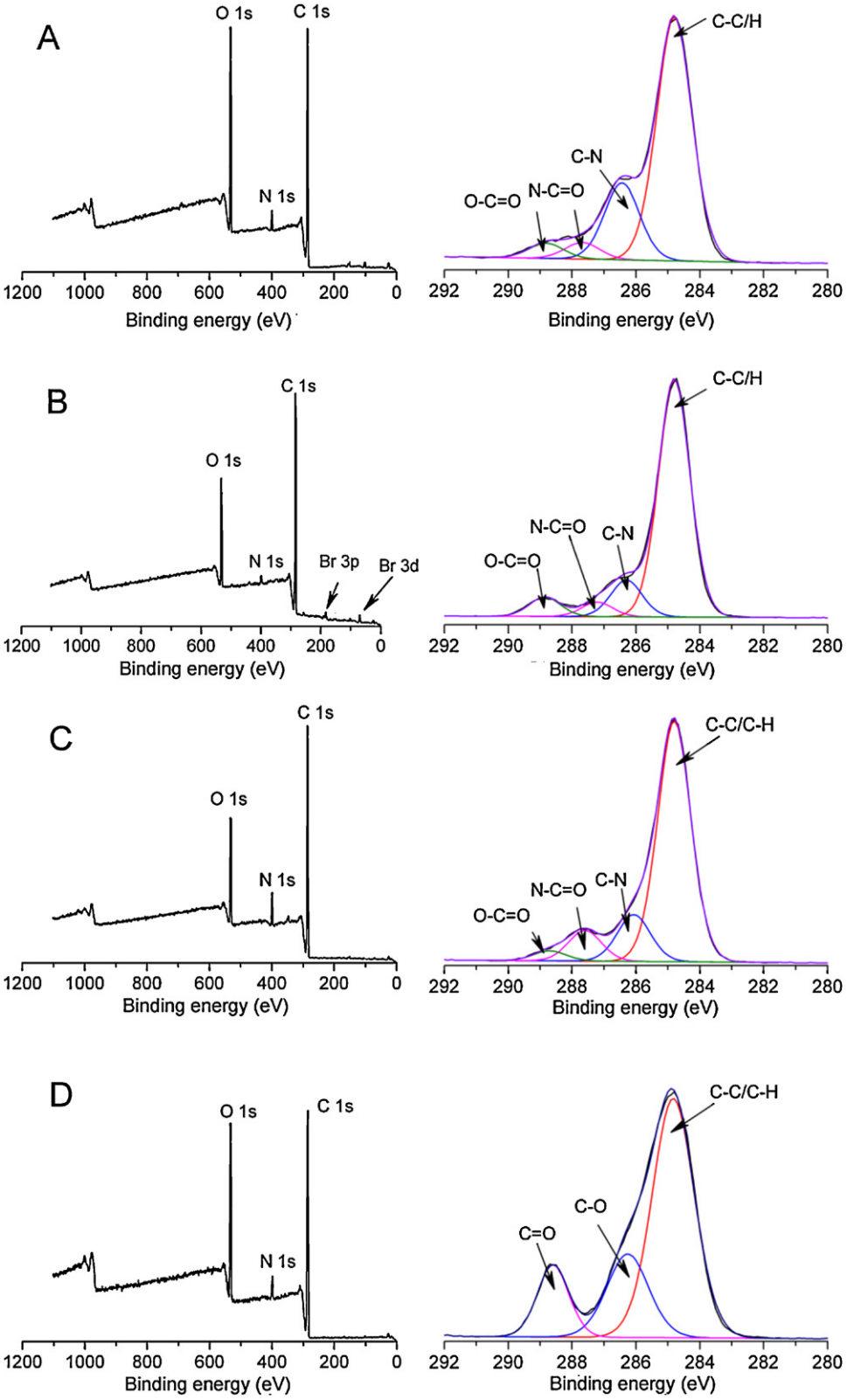

Fig. 3. XPS spectra for CCM (A), BriB–CCM (B), CCM–PNIPAAm (C), and PDEAEMA–CCM (D). The left panel shows the full-scan deconvoluted curves, and the right panel shows the C 1s core level curves.

ARGET ATRP is the use of lower catalyst concentrations than in ATRP (Bhut et al., 2012; Matyjaszewski et al., 2006), as catalyst removal or recycling is a problem in many industrial applications.

3.2. Chemical structure characterizations

Fig. 2 shows the ATR-IR spectra of the membranes at different polymerization stages. The characteristic peaks of CCM were discussed in our previous work (Qiu et al., 2012). Comparing the spectrum of BriB–CCM with that of CCM, a new absorption peak appeared at 1737 cm^{-1} and the peak at 3400 cm^{-1} disappeared. These changes were ascribed to the —COO— groups, which were created by the reaction of —OH groups from MCC with BriB (Wang, Tan, et al., 2011; Wang, Qiu, et al., 2011), and the results suggested that the BriB–CCM macroinitiator was obtained. The spectrum of PNIPAAm–CCM represents the surface of the PDEAEMA–CCM–PNIPAAm membrane grafted with PNIPAAm and that of CCM–PDEAEMA represents the other surface, grafted with PDEAEMA. The characteristic peaks of PNIPAAm at 1652 cm^{-1} and 1544 cm^{-1}, attributed to amide carbonyl groups and tertiary amine groups (Lindqvist et al., 2008; Wandera et al., 2011), were observed in the spectrum of PNIPAAm–CCM. Peaks also appeared at 3288 cm^{-1} and 2970 cm^{-1}, corresponding to the vibrations from the tertiary amine groups and methyl groups of PNIPAAm. In the spectrum of CCM–PDEAEMA, an intense signal at 1727 cm^{-1} was observed, arising from the C=O stretching vibration band of the PDEAEMA side-chains (Wang, Tan, et al., 2011; Wang, Qiu, et al., 2011). In addition, the characteristic C—N stretching vibration band at 1482 cm^{-1} was observed.

The surface compositions of CCM, BriB–CCM, and the two sides of the PDEAEMA–CCM–PNIPAAm membrane were analyzed using XPS, and the results are shown in Fig. 3. The left column shows the full-scan spectra and the right column shows the C 1s high-resolution-scan spectra. The CCM membrane was obtained by crosslinking cellulose with TDI, producing carbamate groups [O—C(O)—N]. Fig. 3A shows that the CCM membrane contained C, N, and O elements, and the binding energies of the four composition components were centered at 284.8 eV, 286.4 eV, 287.7 eV, and 288.8 eV, corresponding to the chemical bonding environments of C—C or C—H, C—N, N—C=O, and O—C=O, respectively. The results conformed fairly well to the chemical structure of the CCM membrane. Fig. 3B shows the XPS spectra of BriB–CCM. Br was observed at around 180 eV and 70 eV, corresponding to Br 3p and Br 3d, respectively (Pan, Hamad, et al., 2010; Pan, Zhang, et al., 2010). Compared with the CCM membrane, the detected amounts of C—N and N element decreased, whereas the amount of O—C=O increased as a consequence of the immobilization of BriB on the surface. These results indicated that the initiator was immobilized on the CCM membrane surface. Fig. 3C and D shows the spectra of each side of the assembled PDEAEMA–CCM–PNIPAAm membrane. The binding energies of the PNIPAAm side in terms of C 1s were found at 284.8 eV, 286.1 eV, 287.6 eV, and 288.7 eV, but the relative quantities of C—N and N—C=O were higher than in BriB–CCM; similar results have already been reported in the literature (Chou, Shih, Tsai, Chiu, & Lue, 2012; Kurkuri, Nussio, Deslandes, & Voelcker, 2008). Regarding the PDEAEMA side, three peak components at binding energies of 284.8 eV, 286.3 eV, and 288.6 eV, ascribed to C—C/H, C—O, and O—C=O, were observed, and this result was in reasonably good agreement with other studies (Fujii et al., 2010; Qiu et al., 2009; Wang, Tan, et al., 2011; Wang, Qiu, et al., 2011), indicating that PDEAEMA was successfully grafted from the surface of BriB–CCM.

Taken together, the XPS and ATR-IR spectra data indicated that the obtained membrane was heterostructured, i.e., one surface of the membrane was grafted with PNIPAAm and the other one was grafted with PDEAEMA.

3.3. Examination of influence of monomer penetration across membranes

To elucidate whether the monomers could penetrate through the BriB–CCM membrane and interfere with each other, experiments with one of the chambers containing NIPAAm or DEAEMA and the other chamber free of monomers were conducted. The structures of PDEAEMA–CCM and CCM–PNIPAAm were each characterized using ATR-IR, XPS, and SEM measurements.

Fig. 4 shows the SEM images of cross-sections of CCM–PNIPAAm (A) and PDEAEMA–CCM (B) membranes. The upper surface of CCM–PNIPAAm was rough, whereas the bottom surface was still flat and neat. In the reaction chamber, the upper surface was the side incubated with the NIPAAm monomer and the other surface was the one with no monomer. In the cross-section morphology of PDEAEMA–CCM (Fig. 4B), we can see that there are many stripes growing from one side of the membrane (lower side), forming a rough surface, and this phenomenon was not found on the opposite side. The chemical structures of these two membranes were confirmed by ATR-IR and XPS. The ATR-IR spectra and XPS (data not shown) demonstrated that the BriB–CCM membrane surface without NIPAAm or DEAEMA added to the chamber retained the same chemical structure as that of the BriB–CCM membrane, whereas the surface with NIPAAm or DEAEMA added was successfully grafted with PNIPAAm or PDEAEMA.

These results suggested that the monomers could not penetrate across the membrane and heterostructured membranes could be obtained without interference. The CCM membrane had intense crosslinked networks and possessed controlled and slow permeation of small molecules (Qiu et al., 2012), thus the monomers could not easily migrate through the membrane. The

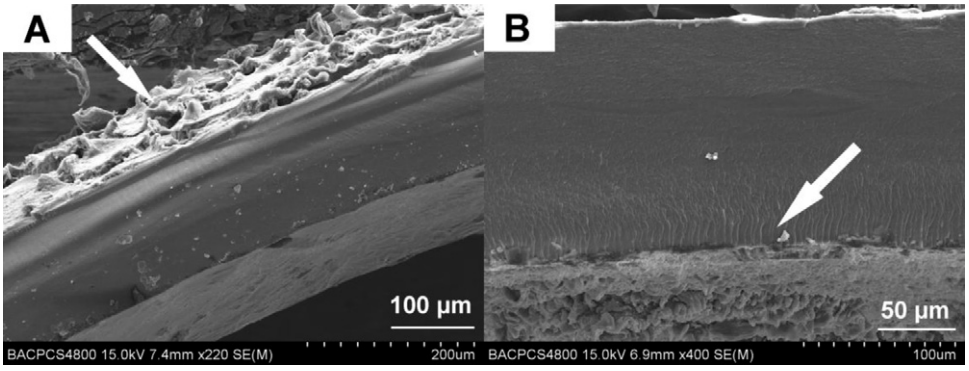

Fig. 4. SEM images of cross-sections of CCM–PNIPAAm (A) and PDEAEMA–CCM (B) membranes.

ATRP polymerization rate is fast and the contribution of termination becomes insignificant as a result of the persistent radical effect (Matyjaszewski & Xia, 2001), so the monomers approaching the membrane surface became involved in reactions instead of penetrating across the membrane into the other chamber. Monomer penetration therefore had a negligible effect on the formation of the PDEAEMA–CCM–PNIPAAm membranes.

3.4. Morphologies and grafting thicknesses of PDEAEMA–CCM–PNIPAAm membranes

The morphologies of the surfaces of CCM, BriB–CCM, and PDEAEMA–CCM–PNIPAAm and the cross-section of PDEAEMA–CCM–PNIPAAm were studied by SEM, and the results are shown in Figs. 5 and 6. The CCM membrane surface was smooth and neat (Fig. 5A), but after reaction with BriB some cracks and holes appeared on the surface (Fig. 5B). The defects were only observed on the surface, and the membrane retained its integrity, according to the cross-section images in Fig. 6. The morphology of PNIPAAm differed from that of PDEAEMA (Figs. 5C, D and 6). The grafted PNIPAAm layer stuck to the membrane compactly, in a gel-like layer, as reported elsewhere (Lue et al., 2011). The structure of the grafted PDEAEMA was relatively loose, and the microview of the polymer growing from the membrane showed continuous strips.

The thicknesses of the grafted polymers were examined using the SEM images shown in Fig. 7. The thicknesses of the PNIPAAm layer and the PDEAEMA layer increased linearly with time, and the PDEAEMA layer was much thicker than the PNIPAAm layer at the same reaction time. The thicknesses of the highly grafted layers reached 12 μm for PNIPAAm and 40 μm for PDEAEMA at 12 h. A well-documented characteristic of controlled, surface-initiated ATRP from a low surface area is a linear relationship between polymer thickness and time (Munirasu, Karunakaran, Rühe, &

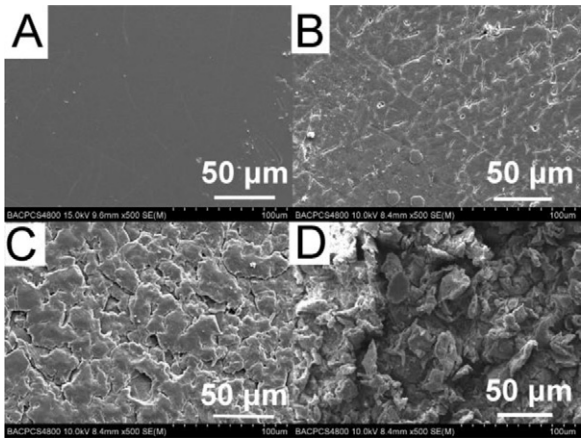

Fig. 5. SEM images of surface morphologies of CCM (A), BriB–CCM (B), CCM–PNIPAAm (C), and PDEAEMA–CCM (D).

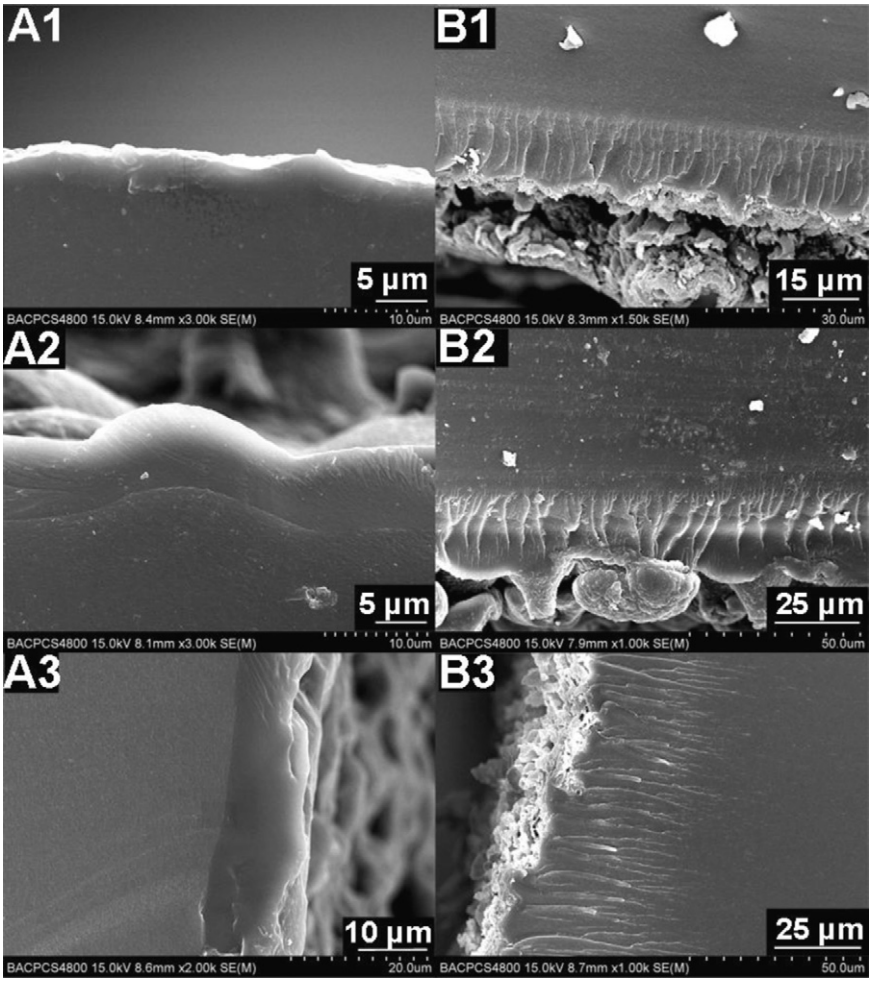

Fig. 6. SEM images of cross-sections of PDEAEMA–CCM–PNIPAAm membranes at different reaction times: 4 h (1), 8 h (2), and 12 h (3). Part (A) shows the side grafted with PNIPAAm, and Part (B) shows the other side, grafted with PDEAEMA.

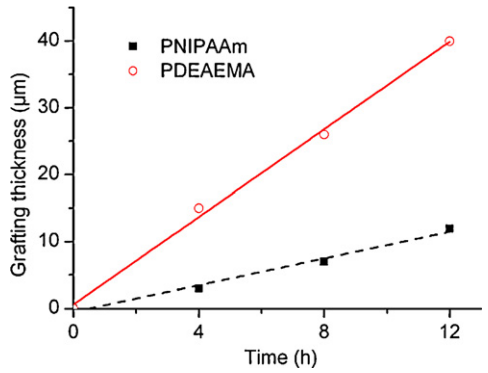

Fig. 7. Grafted polymer thicknesses as a function of reaction time (observed from SEM images of cross-sections of PDEAEMA–CCM–PNIPAAm membranes) for grafted PDEAEMA and grafted PNIPAAm.

Dhamodharan, 2011; Wandera et al., 2011), especially when the radical concentration is low (Behling, Williams, Staade, Wolf, & Cochran, 2009; Kim, Huang, Miller, Baker, & Bruening, 2003; Xiao & Wirth, 2002; Zhou, Gao, Wang, & Zhu, 2012), and this was clearly shown in our results. The NIPAAm monomer was less reactive than the DEAEMA monomer in ATRP, probably because of the methyl on the vinyl group of DEAEMA (Braunecker & Matyjaszewski, 2007; Peng, Kong, Seeliger, & Matyjaszewski, 2011), so the PDEAEMA layer was thicker than the PNIPAAm layer.

3.5. Properties of dual-responsive membranes

Fig. 8 shows the contact angles of both sides of the PDEAEMA–CCM–PNIPAAm membrane (A and B) and the reversibility changes of contact angles responsive to temperature and pH (C). For the side grafted with PNIPAAm, the contact angle exhibited temperature-dependent changes. For example, increasing the temperature from 20 °C to 50 °C, the contact angle increased from 13.0° to 72.8°, and remained essentially unchanged after further temperature increases (Fig. 8A). The PNIPAAm polymer showed a characteristic lower critical solution temperature (LCST) point at around 32 °C in aqueous solution (Schild, 1992), below which it is hydrophilic as a result of efficient hydrogen bonding with water. In contrast, intramolecular hydrogen bonds are formed above the LCST and precipitation of the polymer occurs as a result of its increased hydrophobicity (Lin, Chen, & Liang, 1999; Lindqvist et al., 2008). PNIPAAm brushes showed similar wettability changes with temperature. Further temperature increases above the LCST had a minor influence on the hydrophobicity of the PNIAAm polymer (Schild, 1992), so the contact angle at 80 °C (74.9°) remained the same as that at 50 °C.

On the other side, the PDEAEMA grafted layer revealed pH-dependent behavior (Fig. 8B). Under acidic conditions, the contact angles were 54.6° and 73.6° for pH values of 1.0 and 4.0, respectively. When the pH value was increased to 7.0 and 10.0, the contact angles increased to 136.6° and 131.5°. In aqueous media with pH < 6.5, the tertiary amine groups on the PDEAEMA chain are in a protonated state and the polymer is hydrophilic. In aqueous media with pH > 6.5, PDEAEMA will coagulate as a

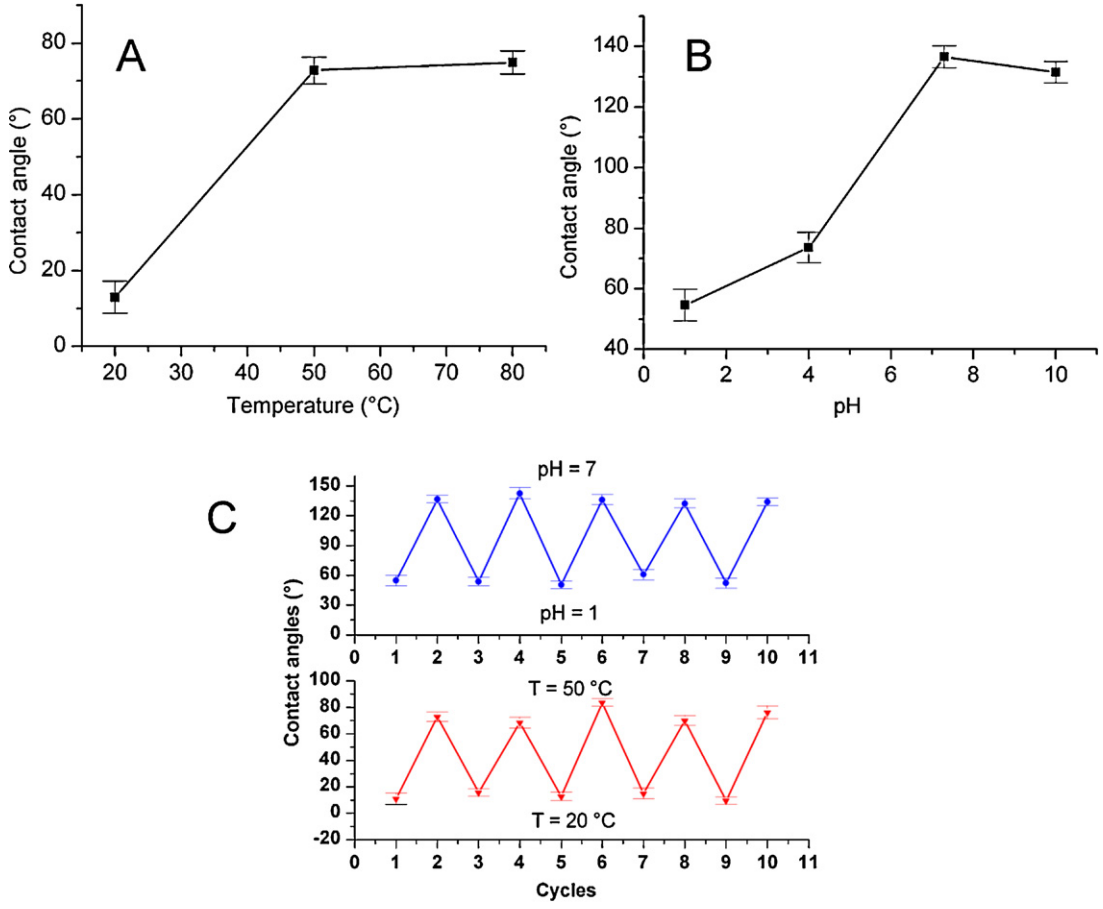

Fig. 8. Water contact angles for surface grafted with PNIPAAm at different temperatures (A), and for surface grafted with PDEAEMA at different pH values (B), and (C): Water contact angles for surface grafted with PNIPAAm at different temperatures (lower): half-cycles, $T = 20$ °C; integral cycles, $T = 50$ °C, and for surface grafted with PDEAEMA at different pH values (upper): half-cycles, pH 1.0; integral cycles, pH 7.0.

result of deprotonation of the tertiary amine groups (Wang, Tan, et al., 2011; Wang, Qiu, et al., 2011). At pH < pK_a, a lower pH will lead to more tertiary amine groups being protonated, thus the PDEAEMA is more hydrophilic, and, in our case, the contact angle of PDEAEMA brushes at pH 1.0 was lower than that at pH 4.0. PDEAEMA can also be permanently quaternized and converted to zwitterionic structures via reaction with propane sultone, forming materials with upper critical solution temperature properties (Lee, Pietrasik, Sheiko, & Matyjaszewski, 2010). This property of PDEAEMA gives rise to various changes in the properties of the PDEAEMA–CCM–PNIPAAm membrane.

To test the reversibility, the contact angles of PDEAEMA–CCM–PNIPAAm were measured on cycling between 20 °C and 50 °C and cycling between pH 1.0 and pH 7.0. Reversible switching between hydrophilic and hydrophobic characters for the PDEAEMA–CCM–PNIPAAm membrane is shown in Fig. 8C. The surface grafted with PNIPAAm showed repeatable temperature-dependent wettability switches between 20 °C and 50 °C, and the surface grafted with PDEAEMA showed reversible switching of pH-dependent wettability between pH 1.0 and pH 7.0. These results were in accordance with those for PNIPAAm- and poly (4-vinylpyridine)-grafted cellulose surfaces (Lindqvist et al., 2008).

4. Conclusions

A novel pH- and temperature-sensitive cellulose membrane was produced by simultaneous grafting of PNIPAAm and PDEAEMA on a crosslinked cellulose membrane. The double-grafting process was simplified by using a diffusion device and ARGET ATRP. A high grafting thickness of the stimuli sensitive polymers was obtained, and the grafted polymer thicknesses increased linearly with reaction time. The PNIPAAm-grafted surface was hydrophilic below the LCST of PNIPAAm, according to the results of water contact angle measurements, whereas this surface was hydrophobic above the LCST. The PDEAEMA-grafted surface showed wettability changes in response to pH changes between acidic and basic conditions. The wettability of the PDEAEMA–CCM–PNIPAAm membrane was reversible on cycling between 20 °C and 50 °C and between pH 1.0 and pH 7.0. This synthesis method allows us to prepare various dual-responsive membranes in a simple way by altering the monomer compositions. The membrane surfaces are heterostructured, with different polymers grafted on each surface, and this dual-responsive cellulose membrane may find potential specific applications in water treatment, separation, drug delivery, etc.

Acknowledgements

This work was supported by the Chinese National Scientific Foundation (21175150) and the National Key Technology R & D Program (2011BAD11B02), by the Ministry of Science & Technology of China.

References

Allen, A. L., Tan, K. J., Fu, H., Batteas, J. D., & Bergbreiter, D. E. (2012). Solute- and temperature-responsive smart grafts and supported membranes formed by covalent layer-by-layer assembly. *Langmuir*, *28*, 5237–5242.

Behling, R. E., Williams, B. A., Staade, B. L., Wolf, L. M., & Cochran, E. W. (2009). Influence of graft density on kinetics of surface-initiated ATRP of polystyrene from montmorillonite. *Macromolecules*, *42*, 1867–1872.

Bhut, B. V., Conrad, K. A., & Husson, S. M. (2012). Preparation of high-performance membranes adsorbers by surface-initiated AGET ATRP in the presence of dissolved oxygen and low catalyst concentration. *Journal of Membrane Science*, *390–391*, 43–47.

Braunecker, W. A., & Matyjaszewski, K. (2007). Controlled/living radical polymerization: Features, developments, and perspectives. *Progress in Polymer Science*, *32*, 93–146.

Cai, G., Gorey, C., Zaky, A., Escobar, I., & Gruden, C. (2011). Thermally responsive membrane-based microbiological sensing component for early detection of membrane biofouling. *Desalination*, *270*, 116–123.

Chen, X., Wu, W., Guo, Z., Xin, J., & Li, J. (2011). Controlled insulin release from glucose-sensitive self-assembled multilayer films based on 21-arm star polymer. *Biomaterials*, *32*, 1759–1766.

Chou, F. Y., Shih, C. M., Tsai, M. C., Chiu, W. Y., & Lue, S. J. (2012). Functional acrylic acid as stabilizer for synthesis of smart hydrogel particles containing a magnetic Fe_3O_4 core. *Polymer*, *53*, 2839–2846.

Fujii, S., Suzaki, M., Nakamura, Y., Sakai, K., Ishida, N., & Biggs, S. (2010). Surface characterization of nanoparticles carrying pH-responsive polymer hair. *Polymer*, *51*, 6240–6247.

Gopishetty, V., Roiter, Y., Tokarev, I., & Minko, S. (2008). Multiresponsive biopolyelectrolyte membrane. *Advanced Materials*, *20*, 4588–4593.

Gordijo, C. R., Koulajian, K., Shuhendler, A. J., Bonifacio, L. D., Huang, H. Y., Chiang, S., et al. (2011). Nanotechnology-enabled closed loop insulin delivery device: In vitro and in vivo evaluation of glucose-regulated insulin release for diabetes control. *Advanced Functional Materials*, *21*, 73–82.

Kaiden, T., Yuba, E., Harada, A., Sakanishi, Y., & Kono, K. (2011). Dual signal-responsive liposomes for temperature-controlled cytoplasmic delivery. *Bioconjugate Chemistry*, *22*, 1909–1915.

Kim, J. B., Huang, W., Miller, M. D., Baker, G. L., & Bruening, M. L. (2003). Kinetics of surface-initiated atom transfer radical polymerization. *Journal of Polymer Science Part A: Polymer Chemistry*, *41*, 386–394.

Kurkuri, M. D., Nussio, M. R., Deslandes, A., & Voelcker, N. H. (2008). Thermosensitive copolymer coatings with enhanced wettabilty switching. *Langmuir*, *24*, 4238–4244.

Lee, H., Pietrasik, J., Sheiko, S. S., & Matyjaszewski, K. (2010). Stimuli-responsive molecular brushes. *Progress in Polymer Science*, *35*, 24–44.

Lin, B. F., Missirlis, D., Krogstad, D. V., & Tirrell, M. (2012). Structural effects and lipid membrane interactions of the pH-responsive GALA peptide with fatty acid acylation. *Biochemistry*, *51*, 4658–4668.

Lin, S. Y., Chen, K. S., & Liang, R. C. (1999). Thermal micro ATR/FT-IR spectroscopic system for quantitative study of the molecular structure of poly(*N*-isopropylacrylamide) in water. *Polymer*, *40*, 2619–2624.

Lindqvist, J., Nyström, D., Östmark, E., Antoni, P., Carlmark, A., Johansson, M., et al. (2008). Intelligent dual-responsive cellulose surfaces via surface-initiated ATRP. *Biomacromolecules*, *9*, 2139–2145.

Liu, S. L., Zeng, J., Tao, D. D., & Zhang, L. N. (2010). Microfiltration performance of regenerated cellulose membrane prepared at low temperature for wastewater treatment. *Cellulose*, *17*, 1159–1169.

Lqbal, J., Kim, H. J., Yang, J. S., Baek, K., & Yang, J. W. (2007). Removal of arsenic from groundwater by micellar-enhanced ultrafiltration (MEUF). *Chemosphere*, *66*, 970–976.

Lue, S. J., Chen, C. H., Shih, C. M., Tsai, M. C., Kuo, C. Y., & Lai, J. Y. (2011). Grafting of poly(*N*-isopropylacrylamide-*co*-acrylic acid) on micro-porous polycarbonate films: Regulating lower critical solution temperatures for drug controlled release. *Journal of Membrane Science*, *379*, 330–340.

Lue, S. J., Hsu, J. J., & Wei, T. C. (2008). Drug permeation modeling through the thermo-sensitive membranes of poly(*N*-isopropylacrylamide) brushes grafted onto micro-porous films. *Journal of Membrane Science*, *321*, 146–154.

Matyjaszewski, K., Coca, S., Gaynor, S. G., Wei, M., & Woodworth, B. E. (1998). Controlled radical polymerization in the presence of oxygen. *Macromolecules*, *31*, 5967–5969.

Matyjaszewski, K., Dong, H., Jakubowski, W., Pietrasik, J., & Kusumo, A. (2007). Grafting from surfaces for everyone: ARGET ATRP in the presence of air. *Langmuir*, *23*, 4528–4531.

Matyjaszewski, K., Jakubowski, W., Min, K., Tang, W., Huang, J., Braunecker, W. A., et al. (2006). Diminishing catalyst concentration in atom transfer radical polymerization with reducing agents. *Proceedings of the National Academy of Sciences of the United States of America*, *103*, 15309–15314.

Matyjaszewski, K., Tsarevsky, N. V., Braunecker, W. A., Dong, H., Huang, J., Jakubowski, W., et al. (2007). Role of Cu^0 in controlled/living radical polymerization. *Macromolecules*, *40*, 7795–7806.

Matyjaszewski, K., & Xia, J. (2001). Atom transfer radical polymerization. *Chemical Reviews*, *101*, 2921–2990.

Munirasu, S., Karunakaran, R. G., Rühe, J., & Dhamodharan, R. (2011). Synthesis and morphological study of thick benzyl methacrylate-styrene diblock copolymer brushes. *Langmuir*, *27*, 13284–13292.

Pan, J., Hamad, W., & Straus, S. K. (2010). Parameters affecting the chiral Nematic phase of nanocrystalline cellulose films. *Macromolecules*, *43*, 3851–3858.

Pan, K., Ren, R., Li, H., & Cao, B. (2012). Preparation of dual stimuli-responsive PET track-etched membrane by grafting copolymer using ATRP. *Polymer for Advanced Technologies*, http://dx.doi.org/10.1002/pat.3044

Pan, K., Zhang, X., Ren, R., & Cao, B. (2010). Double stimuli-responsive membranes grafted with block copolymer by ATRP method. *Journal of Membrane Science*, *356*, 133–137.

Peng, C.-H., Kong, J., Seeliger, F., & Matyjaszewski, K. (2011). Mechanism of halogen exchange in ATRP. *Macromolecules*, *44*, 7546–7557.

Qiu, J., Wang, Z., Li, H., Xu, L., Peng, J., Zhai, M., et al. (2009). Adsorption of Cr(VI) using silica-based adsorbent prepared by radiation-induced grafting. *Journal of Hazardous Materials*, *166*, 270–276.

Qiu, X., Tao, S., Ren, X., & Hu, S. (2012). Modified cellulose films with controlled permeatability and biodegradability by crosslinking with toluene diisocyanate under homogeneous conditions. *Carbohydrate Polymers*, *88*, 1272–1280.

Schild, H. G. (1992). Poly(*N*-isopropylacrylamide): Experiment, theory and application. *Progress in Polymer Science*, *17*, 163–249.
Schmid, C., Weidner, S., Falkenhagen, J., & Barner-Kowollik, C. (2012). In-depth LCCC-(GELC)-SEC characterization of ABA block copolymers generated by a mechanistic switch from RAFT to ROP. *Macromolecules*, *45*, 87–99.
Schmitt, F., Granet, R., Sarrazin, C., Mackenzie, G., & Krausz, P. (2011). Synthesis of anion exchange membranes from cellulose: Crosslinking with diiodobutane. *Carbohydrate Polymers*, *86*, 362–366.
Shaikh, R. P., Pillay, V., Choonara, Y. E., du Toit, L. C., Ndesendo, V. M. K., Bawa, P., et al. (2010). A review of multi-responsive membranous systems for rate-modulated drug delivery. *AAPS PharmSciTech*, *11*, 441–459.
Tokarev, I., & Minko, S. (2009). Multiresponsive, hierarchically structured membranes: New, challenging, biomimetic materials for biosensors, controlled release, biochemical gates, and nanoreactors. *Advanced Materials*, *21*, 241–247.
Wandera, D., Wickramasinghe, S. R., & Husson, S. M. (2011). Modification and characterization of ultrafiltration membranes for treatment of produced water. *Journal of Membrane Science*, *373*, 178–188.
Wang, D., Tan, J., Kang, H., Ma, L., Jin, X., Liu, R., et al. (2011). Synthesis, self-assembly and drug release behaviors of pH-responsive copolymers ethyl cellulose-graft-PDEAEMA through ATRP. *Carbohydrate Polymers*, *84*, 195–202.
Wang, N., Zhang, G., Ji, S., Qin, Z., & Liu, Z. (2010). The salt-, pH- and oxidant-responsive pervaporation behaviors of weak polyelectrolyte multilayer membranes. *Journal of Membrane Science*, *354*, 14–22.
Wang, Y., Qiu, J., Peng, J., Xu, L., Li, J., & Zhai, M. (2011). Study on the chemical stability of the anion exchange membrane of grafting dimethylaminoethyl methacrylate. *Journal of Membrane Science*, *376*, 70–77.
Weiss, J., & Laschewsky, A. (2012). One-step synthesis of amphiphilic, double thermoresponsive diblock copolymers. *Macromolecules*, *45*, 4158–4165.
Wu, J. J., Liang, S. M., Dai, H. G., Zhang, X. Y., Yu, X. L., Cai, Y. L., et al. (2010). Structure and properties of cellulose/chitin blended hydrogel membranes fabricated via a solution pre-gelation technique. *Carbohydrate Polymers*, *79*, 677–684.
Xiao, D., & Wirth, M. J. (2002). Kinetics of surface-initiated atom transfer radical polymerization of acrylamide on silica. *Macromolecules*, *35*, 2919–2925.
Xiong, X., Duan, J., Zou, W., He, X., & Zheng, W. (2010). A pH-sensitive regenerated cellulose membrane. *Journal of Membrane Science*, *363*, 96–102.
Yi, Z., Zhu, L. P., Xu, Y. Y., Li, X. L., Yu, J. Z., & Zhu, B. K. (2010). F127-based multiblock copolymer additives with poly(*NN*-dimethylamino-2-ethyl methacrylate) end chains: The hydrophilicity and stimuli-responsive behavior investigation in polyethersulfone membranes modification. *Journal of Membrane Science*, *364*, 34–42.
Zhang, G., Song, X., Ji, S., Wang, N., & Liu, Z. (2008). Self-assembly of inner skin hollow fiber polyelectrolyte multilayer membranes by a dynamic negative pressure layer-by-layer technique. *Journal of Membrane Science*, *325*, 109–116.
Zhang, Z. B., Zhu, X. L., Xu, F. J., Neoh, K. G., & Kang, E. T. (2009). Temperature- and pH-sensitive nylon membranes prepared via consecutive surface-initiated atom transfer radical graft polymerizations. *Journal of Membrane Science*, *342*, 300–306.
Zhao, C., Nie, S., Tang, M., & Sun, S. (2011). Polymeric pH-sensitive membranes—a review. *Progress in Polymer Science*, *36*, 1499–1520.
Zhou, D., Gao, X., Wang, W., & Zhu, S. (2012). Termination of surface radicals and kinetic modeling of ATRP grafting from flat surface by addition of deactivator. *Macromolecules*, *45*, 1198–1207.